

INTRODUCTION

Tidal inlets and their impacts on adjacent shorelines have become a primary focus of coastal research in North Carolina. This focus is primarily due to the state's need to control oceanfront beach erosion and regulate development within poorly defined inlet hazard zones. Of the 20 diverse tidal inlets that exist along the North Carolina coastline, 16 are located south of Cape Lookout and 13 border developed barriers. As a result, most inlets have experienced some form of modification ranging from minor interior channel maintenance to complete stabilization involving extensive dredging or the construction of hard structures. Erosion along adjacent shoreline segments has recently been exacerbated due to the influence of recent storm activity in concert with natural shoreline response to adjusting inlet morphologies. Consequently, tidal inlets, regardless of size, have been targeted as sand resources for potential beach-fill projects. Alterations associated with the removal of large amounts of beach fill material from a particular inlet system may have negative impacts on inlet sand bodies, adjacent oceanfront shorelines, and large-scale circulation patterns. Inlet influence on adjacent shorelines is essentially controlled by the existing hydraulics of the system. Significant change to inlet parameters such as tidal prism and current dominance may have dramatic impacts on ebb-tidal delta retention capacity and hence, oceanfront shoreline response. Ultimately, these alterations may lead to increased rates of oceanfront shoreline erosion.

In order to understand the potential impacts associated with the aforementioned alterations, the establishment of baseline hydrographic data is

necessary. The extent to which an inlet system interrupts longshore transport and temporarily stores sand in the inlet throat and the ebb-tidal delta depends largely upon the wave climate and the inlet's hydrography (NUMMEDAL, et al., 1977; HAYES, 1980; FITZGERALD, 1996; HAYES, 1994). Therefore, knowledge of how dredging alters an inlet's physical parameters, current dominance, and basin filling characteristics is critical to developing an effective inlet management plan. In order to better predict the impact of any future modification to an inlet system, an understanding of the inter-relationships between inlet hydrography, its sand bodies, and oceanfront shoreline change is critical. These data are essential for management purposes and for evaluation of potential impacts produced by alteration of the inlet system.

Knowledge concerning hydraulic parameters and basin filling characteristics for most of North Carolina inlets is lacking. This is the case for Rich Inlet, located in southeastern North Carolina, approximately 55km northeast of Cape Fear. This investigation was designed to provide a pre-modification framework for monitoring future dredging projects. Rich Inlet will likely be the site of future extensive dredging efforts for major beach fill projects on Figure Eight Island, a privately developed barrier located immediately to the southwest (Fig 1 and 2).

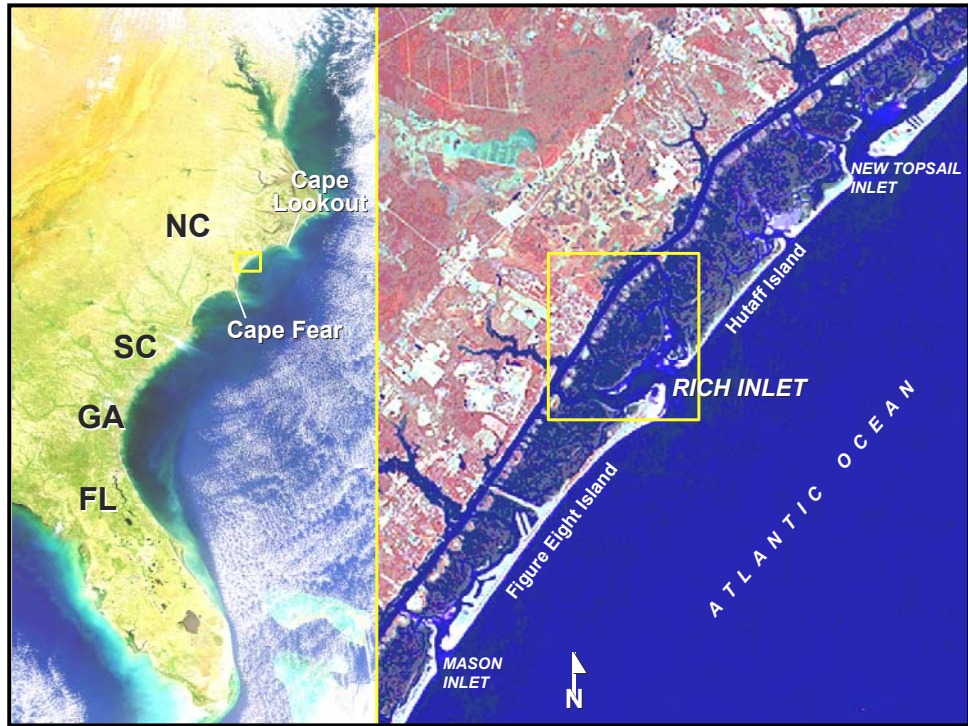


Figure 1. Location map of the study area.



Figure 2. Orthophoto (1993 DOQQ) of the Rich Inlet system, including Nixon and Green Channels and the AIWW.

BACKGROUND

Previous works addressing tidal inlet hydraulics are numerous, but they have generally not included the use of Acoustic Doppler Current Profilers (ADCP). Traditional engineering studies are the basis for modern ADCP instrumentation and software. These studies (ESCOFFIER, 1940; KEULEGAN, 1951; VAN DE KREEKE, 1967; BRUUN, 1968; O'BRIEN, 1969; WALTON and ADAMS, 1976; JARRETT, 1976) and their associated current, flow, and tide calculation equations serve as the foundation for ADCP-generated data. The aforementioned studies also provided the basis for further understanding of tidal inlet systems and associated hydraulic processes through their empirical based approaches. However, many of the formulated models cannot answer management-oriented questions about a particular system without details of local variables (CLEARY, 1996). Site-specific investigations are necessary in order to further understand tidal inlet behavior. A relevant point was expressed by FITZGERALD (1996) who emphasized that although significant amounts of information concerning tidal inlets has been published, it is difficult to predict how a particular inlet will behave in response to changes in site-specific variables.

A number of inlet studies have been conducted in North Carolina; however they are somewhat broad in scope and address a variety of issues. The U.S. Army Corps of Engineers (USACE) has conducted many of these studies focusing on dredging effects and the construction of navigation improvements such as jetty placement in Masonboro Inlet (VALLIANOS, 1975; USACE, 1982) and Oregon Inlet (USACE, 1999). Other studies (e.g. CLEARY and HOSIER,

1979, 1993; CLEARY and MARDEN, 1999; JOHNSEN et al., 1999) have investigated inlet distribution and their geologic significance along with additional studies, which used aerial photography and spatial analyses to investigate inlet-related channel, sandbody, and shoreline changes (LANGFELDER et al., 1974; BAKER, 1977; CLEARY and MARDEN, 1999).

There are many recent papers that examine tidal inlet hydrographies but few have included the use of ADCP technology. The few existing ADCP-oriented studies vary with slight differences in instrument applications and objectives. Recent ADCP oriented studies have typically used fixed-mounted instruments as opposed to the vessel-mounted application that was used in this study. Notable hydrographic studies that utilized fixed-mounted instruments include the Shinnecock Inlet Site Investigation conducted by the USACE (MILITELLO and KRAUS, 2001) and monitoring conducted by the USACE as part of the Wilmington Harbor Project (MCNINCH, 2002). The Shinnecock Inlet study focused on the identification of tidal and hydrodynamic parameters within the inlet and adjacent waterways. This study concluded that the inlet was flood dominant with greater flood current velocities than those measured during ebb flow. The study also found inequalities between flood and ebb flow volumes or tidal prism (T_p). Volume differences associated with the ebb and flood portions of the tide were attributed to the water level being out of phase with the tidal current. The Shinnecock investigation's objectives were closely related to those of this project, and sought to characterize inlet hydraulics used in the identification of potential impacts associated with alterations to the system.

The benefits associated with the use of a fixed-mounted instrument are that it usually requires little manpower after actual deployment and is beneficial in collecting detailed long-term hydraulic data. However, fixed-mounted instruments are typically unable to collect detailed channel dimensional data and are fairly difficult, as well as costly, to move from one monitoring location to another. Due to this study's objectives and environmental conditions, a vessel-mounted ADCP was utilized to provide several distinct advantages. These advantages include obtaining data pertaining to channel shape, cross-sectional area, channel width, and depth. The vessel-mounted ADCP also allowed for the collection of data at a number of transect locations during a specific survey period.

Studies involving use of a vessel-mounted ADCP include the Rudee Inlet Management Study conducted by Waterway Surveys and Engineering (WSE), Ltd (2001), a preliminary report by the USACE examining the mean current flow across Oregon Inlet (MCNINCH, 2003), portions of the previously mentioned Wilmington Harbor Project (MCNINCH, 2002), and a recent Environmental Assessment investigation for the relocation of Mason Inlet. The latter involved a brief ADCP-based hydrographic examination of Rich, Mason, and Masonboro Inlets conducted by Applied Technology Management (ATM, 1999). Of these studies, the Rudee Inlet study (WSE, 2001) and the Environmental Assessment of Mason Inlet (ATM, 1999) are most similar to the methodology and objectives of this investigation. The Oregon Inlet investigation and monitoring conducted for the Wilmington Harbor Project focused exclusively on examining currents and

tidal prism within each study area. These studies did not focus on monitoring change in relation to tidal amplitude and inlet channel dimensions.

The only comparable ADCP based study conducted along the Onslow Bay portion of the North Carolina coast was the brief two-day ADCP analysis of Masonboro, Mason, and Rich Inlets conducted as part of the Environmental Assessment for the Mason Inlet Relocation Project (ATM, 1999). The objective of this project was to gain a broad understanding of discharge volumes for each of the three inlets using ADCP data (ATM, 1999). Study results indicated that the ebb and flood tidal prisms at Mason Inlet were $6.71 \times 10^5 \text{ m}^3$ and $7.19 \times 10^5 \text{ m}^3$, respectively. Detailed velocity and discharge data were not reported, making the determination of flood or ebb dominance impossible. The ATM surveys conducted at Rich Inlet consisted of three one-quarter tidal cycle (6 hr and 12.5 min) analyses. Spring and neap variations and flood or ebb dominance determination were not addressed.

Aside from peripheral data gathered by ATM, studies specifically addressing the hydrography of Rich Inlet or the majority of North Carolina inlets are non-existent. Lack of information concerning tidal inlet parameters has prompted this study. Data derived from this investigation will serve as a baseline for the development of an effective management strategy for the inlet.

OBJECTIVES

The objectives of this study are to characterize Rich Inlet based on a series of hydrographic parameters, to gain an understanding of the physical

exchange processes under a variety of environmental conditions, and to define the dominant sediment transport pathways. The primary objectives of this study are:

- 1) Collect baseline inlet morphology and flow data.
- 2) Determine velocity, discharge, and tidal prism for varying tidal conditions including neap, mean, and spring conditions.
- 3) Determine flood or ebb dominance through examination of velocity and duration data.
- 4) Estimate ebb-tidal delta retention capacity.
- 5) Determine sediment type and distribution within the inlet throat and primary feeder channels.

The flow data included in this study are average flow velocities, discharge, tidal range (R), lags, and tidal prism (Tp). Data pertaining to the inlet throat dimensions included inlet minimum width (IMW), cross-sectional area (Ac), and depth. Morphologic data were also collected within the feeder channels adjacent to the inlet throat and Atlantic Intracoastal Waterway (AIWW).

For purposes of this study, maximum flow velocity is defined as the maximum velocity recorded during an ADCP survey. Maximum discharge is the maximum value recorded during an individual survey, and Tp is defined as the volume of water that enters an inlet on a spring flood tide. In addition to the Tp values derived from measured discharge, estimates of tidal prism were made using a number of empirical methods, which are examined in the Tidal Prism section of this document.

SITE DESCRIPTION

Rich Inlet is a large wave-influenced transitional system that separates Hutaff Island, a 9 km (5.6 mi) long undeveloped barrier located to the northeast, from Figure Eight Island, a 9 km (5.6 mi) long barrier located to the southwest (Fig. 1). The inlet is backed by a fairly expansive marsh-filled basin where two large tidal creeks, Nixon and Green Channels (Fig. 2), connect the inlet to the AIWW.

Rich Inlet is considered to be a relatively stable system and has migrated very little over the past two centuries. The underlying Tertiary rock units that rise within 5 m (16 ft) of the lagoon surface have played a primary role in confining the inlet's location to a 1 km (3,280 ft) migration pathway. Oligocene siltstone hardbottoms are common along the outer margins of the ebb-tidal delta in water depths of 9 m (-30 ft) (CLEARY, 2001). The ultimate origin of the inlet is probably related to the ancestral channel of Pages Creek, which controlled its location as sea level rose during the past several thousand years. The large drainage area, which includes portions of the bar built lagoon and Pages Creek estuary, enhances the inlet's stability.

Average wave height and period for the region are 0.79 m (2.6 ft) and 7.9 seconds (JARRETT, 1977). The dominant direction of wave approach is from the northeast and east and accounts for approximately 64% of the wave energy impinging on the coast. The USACE (1982) estimated that the gross littoral transport for nearby Wrightsville Beach is 843,150 m³/y (1,095,000 yd³/y) with a net southerly component of 592,130 m³/y (769,000 yd³/y).

METHODOLOGY

This investigation included the collection of detailed hydrographic, sedimentological, and tidal data. Tidal data were collected at four stations where Remote Data Systems Ecotone-80 model water-level meters were installed (Fig. 3). All water-level data were referenced vertically (NGVD '29) and horizontally (North Carolina State Plane 1983). Water-level readings were collected at a frequency of 10 min and recorded within an internal data logger. Post processing of all tidal data consisted of importing readings into a Microsoft Excel spreadsheet for manipulation and analysis. Analyses involved filtering the data for successive high and low waters and the identification of tidal parameters for the study period including Mean High Water (MHW), Mean Sea Level (MSL), Mean Low Water (MLW); neap, average, and spring tidal ranges (tr); lag times; and flood/ebb current durations.

Flow data were collected using a vessel-mounted RD Instruments Workhorse Monitor Broadband 1200kHz ADCP. Long-term deployment of a bottom-mounted ADCP was impossible due to the dynamics of the inlet throat and heavy boat traffic through the interior feeder channels. Preliminary site investigations indicated the presence of large-scale bedforms in the channel thalwegs. The speculated movement of large volumes of material through the inlet throat made instrument burial a likely event. ADCP surveys were conducted in two phases.

Initial ADCP work was conducted along ten channel transects to characterize morphologic variability within the channel network (Fig. 3). Data

were collected for the purpose of characterizing channel depth and shape. The surveys were conducted on 2/14/01, 3/1/01, 6/19/01, and 8/6/01. The second phase of surveys was restricted to the inlet throat; these repetitive throat surveys were focused on collection of detailed flow data for one-half (12 hr 25 min) and one-quarter (6 hr and 12.5 min) tidal cycles. The surveys were conducted at the inlet's minimum width (IMW) along Transect 5 (Fig. 3) in order to measure variations in the tidal prism, discharge, flood/ebb current velocity, flood/ebb duration, inlet minimum width, and cross-sectional area. Throat surveys were conducted on seven separate occasions (Tables 4 and 5). Three of the seven throat surveys captured one-quarter tidal cycles (6 hr and 12.5 min), and the remaining four surveys captured one-half tidal cycles (12 hr and 25 min) (Table 1). Each throat survey was conducted during varying conditions of tidal amplitude. Table 1 lists tidal range information pertaining to each survey date. Because environmental conditions prohibited long-term instrument deployment, snapshot surveys capturing one-quarter and one-half tidal cycles were deemed appropriate and necessary to accurately characterize flow characteristics.

ADCP data acquisition and manipulation were conducted using RDI's WinRiver software (PULAWSKA, 1999) and Microsoft Excel. ESRI Arcview GIS version 3.2 was used to manipulate and display referenced data. The RDI ADCP command setup depended on specific survey-site conditions including maximum depth, suspended sediment concentrations, and flow characteristics. All ADCP data were obtained in instrument Water Mode 1, which was recommended for fast moving water of all depths. Field conditions required modifications to some

of the ADCP setup commands. The default command settings were used for all commands except depth cell number and size, blanking distance, and salinity. Depth cell size and blanking distance was set to 25 cm (0.82 ft), depth cell number was dependent upon depth, and salinity was set to 35 ppt. Discharge measurements were averaged for top and bottom portions of the channel cross-section using CHEN'S (1994) power law coefficient of 0.1667. Bank edge estimates were made assuming that the shape of the area between the channel bank and last good ensemble was triangular. For purposes of this study, IMW is defined as the inlet minimum width at mean low water, tidal prism is the volume of water entering an inlet on a spring flood tide, and inlet cross-sectional area is the channel cross-sectional area at the IMW at mean tide level (MTL). The term "average" is defined as the mean.

Sediment samples were collected using a Wildco Petite Ponar grab sampler to provide information concerning channel sediment types. Ninety-seven samples were collected on three separate sampling surveys (2/14/01, 8/9/01, 9/4/02). Samples were initially collected along each of the ten ADCP transects for purposes of characterizing the sediment type and distribution. The second survey focused on sample collection within a recently dredged area located within Nixon Channel. The third survey consisted of sample collection along each of the ten ADCP transects and within the dredged channel segment in Nixon Channel. The 97 samples were split into ~50 g subsamples and oven dried at 50°C for 24 hrs. The samples were sieved on a Janke and Kunkel KS-500 sieve shaker using U.S. standard sieves, numbers 5, 10, 18, 35, 60, 120,

and 230. Data were entered into a GRADISTAT (BLOTT and PYE, 2001) template in Microsoft Excel for grain size analysis. GRADISTAT statistics were based on FOLK and WARD's classification scheme (1957).

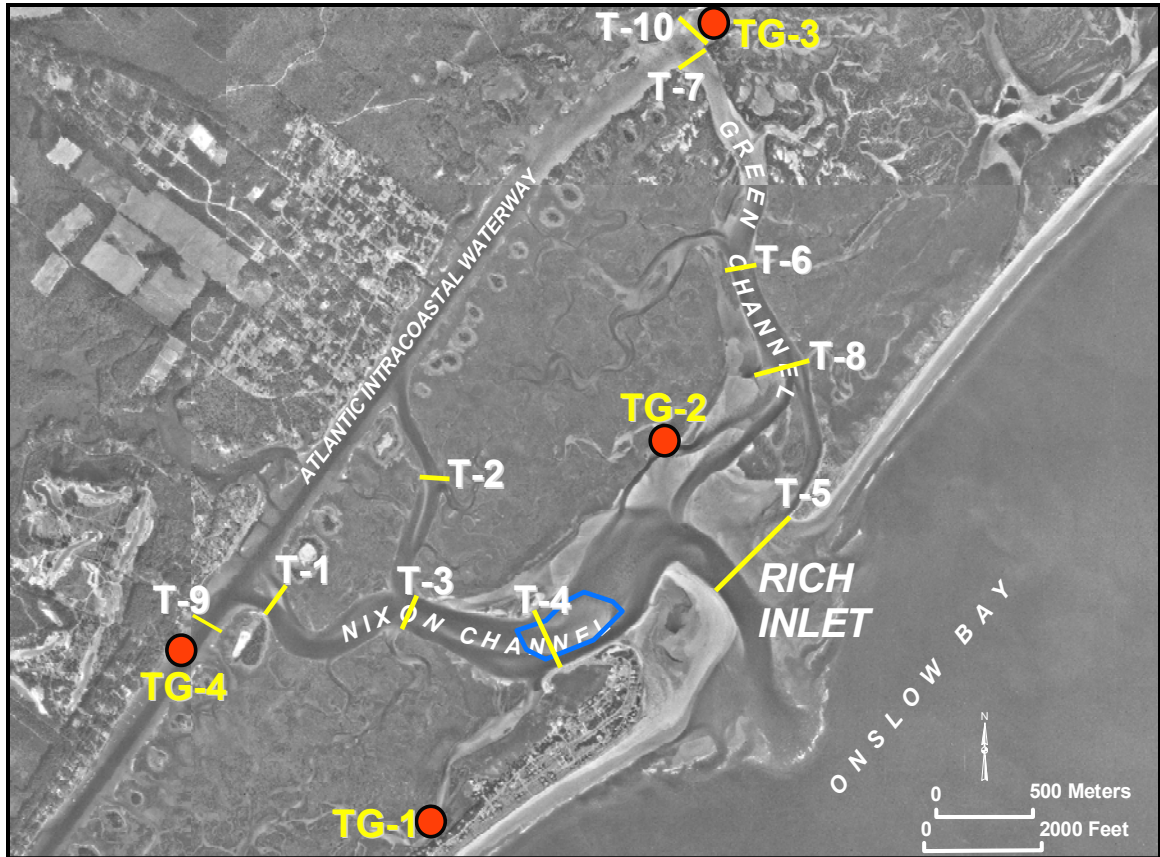


Figure 3. Orthophoto depicting locations of ADCP transects (T) and water-level meters (TG).

Rich Inlet ADCP Surveys				
Date	Survey Type	Tidal Condition	Predicted Flood Range (ft)	Predicted Ebb Range (ft)
2/14/2001	10 transect system survey	Neap Tide (1 day prior)	3.3	3.3
3/1/2001	10 transect system survey	Neap Tide (2 days prior)	2.9	3.1
6/19/2001	10 transect system survey	Spring Tide (2 days prior)	4.6	3.5
8/6/2001	10 transect system survey	Spring Tide (2 days post)	3.3	3.3
10/17/2001	7 hour throat survey	Spring Ebb (1 day post)	4.8	5.3
11/30/2001	7 hour throat survey	Spring Ebb	3.5	4.3
12/7/2001	7 hour throat survey	Neap Flood	3.8	3.9
1/16/2002	13 hour throat survey	Spring Flood and Ebb (3 days post)	3.1	3.8
5/24/2002	13 hour throat survey	Spring Flood and Ebb (2 days prior)	5.2	4.4
7/24/2002	13 hour throat survey	Spring Flood and Ebb	4.6	3.6
10/8/2002	13 hour throat survey	Spring Flood and Ebb (2 days post)	5.5	5.3

Table 1. Tidal conditions and predicted ranges for individual ADCP surveys. Predicted ranges are based on NOAA station at Charleston, SC.

RESULTS

Inlet Throat Dimensional Data

During the course of the investigation, the morphology of the inlet throat changed due to spit growth and recession. Data derived from repetitive throat surveys conducted on 10/17/2001, 11/30/2001, 12/7/2001, 1/16/2002, 5/24/2002, 7/24/2002, and 10/8/2002 indicated that variations in the channel alignment resulted in significant change within the inlet throat. The IMW, during the study period, ranged from 197.2 m to 277.1 m (647 – 909 ft). The average maximum throat depth was ~11 m (36 ft) and ranged from ~10.7 m to 11.3 m (35 to 37 ft) (NGVD '29). The average IMW during the study was 247.2 m (811 ft). Survey data also indicated that the cross-sectional area of the inlet throat was variable, ranging from 1,133.1 m² (12,197 ft²) to 1,353.4 m² (14,568 ft²). The average cross-sectional area was 1,252.5 m² (13,482 ft²). Orientation of the ebb channel fluctuated from 116° (2/01) to 161° (5/02) (JACKSON and CLEARY, 2003). As a

result of the northeasterly deflection of the ebb channel and the associated change in the dimensions of the marginal flood channels, severe erosion occurred along the Figure Eight Island shoulder and downdrift shoreline.

Water-Level Data

Data obtained from water-level meters were used to calculate various tidal parameters including ranges, durations, and lagtimes throughout the system. Tidal ranges were determined by filtering the data for successive high and low water and then resolving the height difference between the corresponding water levels. Range data were then regressed against the predicted tidal ranges for Masonboro Inlet (Fig. 4) (based on NOAA station at Charleston, SC) located 15 km (~9.4 mi) to the southwest. These data suggest that the tidal ranges measured near the Rich Inlet throat agreed well with those predicted for nearby Masonboro Inlet.

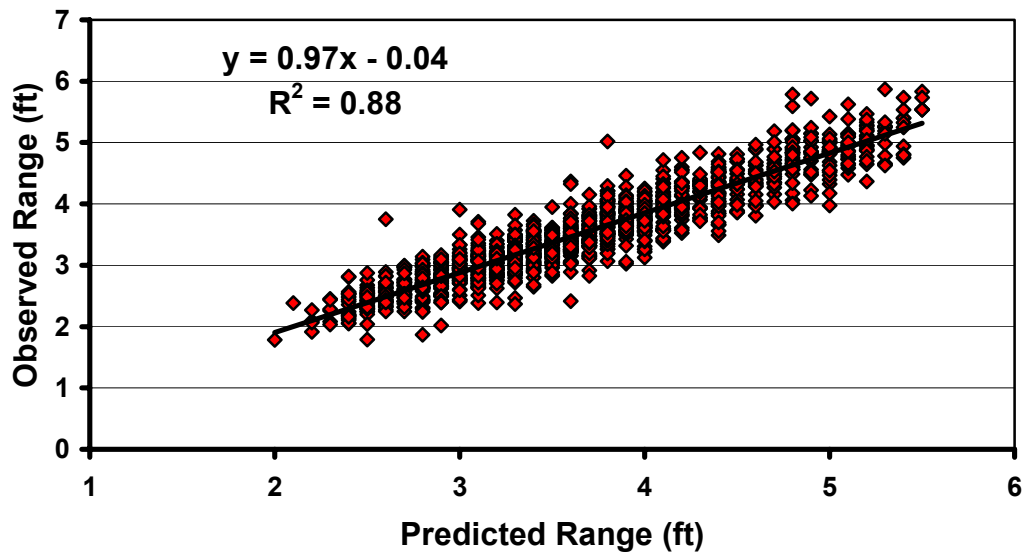


Figure 4. Relationship between predicted tidal ranges at Masonboro Inlet and the measured tidal ranges at TG-2.

Tidal parameters including MHW, MLW, mean range, flood/ebb duration, and lag times for each of the four water-level meters are listed in Table 2. The data indicated that a decrease in tidal range occurred with distance from the inlet throat. Tide gauge 2 (TG-2), located landward of the inlet throat, recorded an average range of 1.08 m (3.54 ft). TG-1, TG-3, and TG-4, located within the backbarrier portions of the system, recorded average ranges of 1.0, 0.97, 1.08 m (3.28, 3.18, 3.54 ft), respectively. Recorded ranges were appreciably less than the average predicted tide range for Masonboro Inlet (1.16 m [3.8 ft]). Differences between recorded ranges for Rich Inlet and those predicted for Masonboro Inlet are most likely attributable to dampening of the tidal wave as it moves through the shallow interior channels behind Rich Inlet. Due to channel friction, a decrease in tidal range is expected with distance from the inlet throat. However, degrees of tidal wave dampening vary depending upon channel shape, bed roughness, depth, and channel orientation (AUBREY and SPEER, 1985; LINCOLN and FITZGERALD, 1988).

Water-Level Meter	Throat (TG-2)	Tidal Creek (TG-1)	Waterway North (TG-3)	Waterway South (TG-4)
Mean High Water Elevation (NGVD '29) (m)	0.96	0.9	N/A	N/A
Mean Low Water Elevation (NGVD '29) (m)	-0.12	-0.1	N/A	N/A
Mean Range (m)	1.08	1	0.97	1.08
Mean Flood Duration (hr)	5.63	5.65	6.03	6
Mean Ebb Duration (hr)	6.78	6.83	6.38	6.4
Mean Lag Time (hr)	N/A	0.58	0.23	0.1

Table 2. Tide gauge statistics for the study period (3/2001-10/2002). Cells marked with N/A depict values, which are unavailable due to error associated with local benchmark.

The mean tidal range recorded at TG-4 (1.08 m [3.54 ft]) was comparable to the mean tidal range measured at the throat (1.08 m [3.54 ft]). These data indicate that tidal range changes little between the throat and the junction of Nixon Channel and the AIWW. A decrease in tidal range was observed between TG-2 (1.08 m [3.54 ft]) and TG-3 (0.97 m [3.18 ft]) located at the junction of Green Channel and the AIWW (Fig. 5). This decrease in tidal range is most likely associated with increased channel friction caused by flow through a shallower, less efficient Green Channel. These data suggest that Nixon Channel is the dominant feeder channel (Fig. 5) in this system. Differences in channel shape, depth, and cross-sectional area of Nixon and Green channels have been documented and are discussed in the Channel Characteristics section of this study.

Flood and ebb durations were determined by resolving the time difference between successive high and low waters. These data indicate that increases in ebb flow durations occurred with proximity to the inlet throat (Table 2). Data from all tide gauge stations showed that the inlet system was flood dominant. This was evident upon inspection of the duration data, which indicated that all water-level meters recorded shorter flood durations hence greater velocities. It is assumed in this case that an equal volume of water is entering as exiting the system during a complete tidal cycle. Data collected at TG-2 (near inlet throat) recorded an average flood duration of 5.63 hr and an average ebb duration of 6.78 hr. Similar values were observed at TG-1, located in a tidal creek immediately behind Figure Eight Island, which recorded a mean flood duration of

5.65 hr and a mean ebb duration of 6.83 hr. Mean flood duration decreased with proximity to the inlet throat (Fig. 6, Table 2). Instruments at TG-3, located at the junction of Green Channel and the AIWW, and TG-4, located at the junction of Nixon Channel and the AIWW, recorded average flood durations of 6.03 hr and 6.0 hr, respectively. Flood current durations at sites TG-3 and TG-4 were appreciably greater than those recorded at TG-1 and TG-2 located near the inlet throat (Fig. 6 and Table 2).

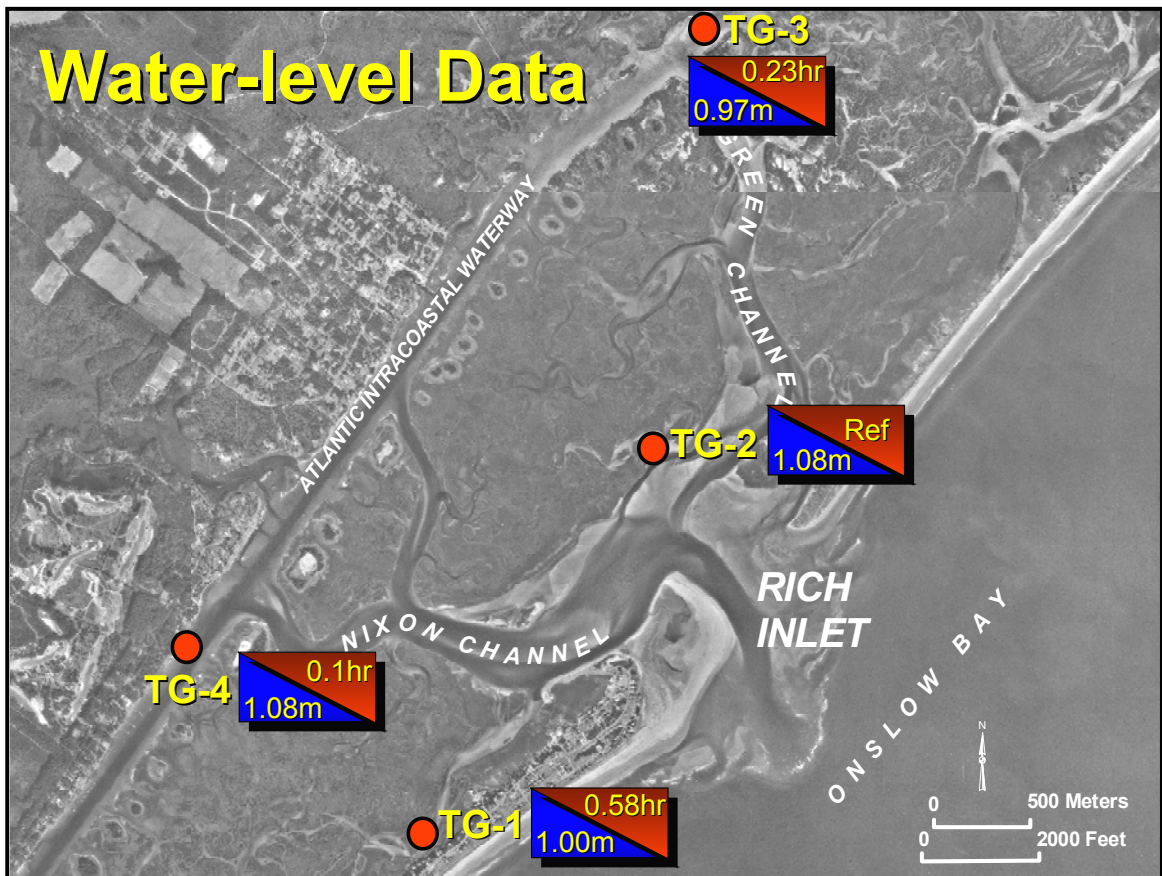


Figure 5. Aerial photograph (1993 DOQQ) showing measured tidal range (blue) and average lag time (red) for each of the four water-level meters. TG-2 was used as reference for the calculation of lag times.

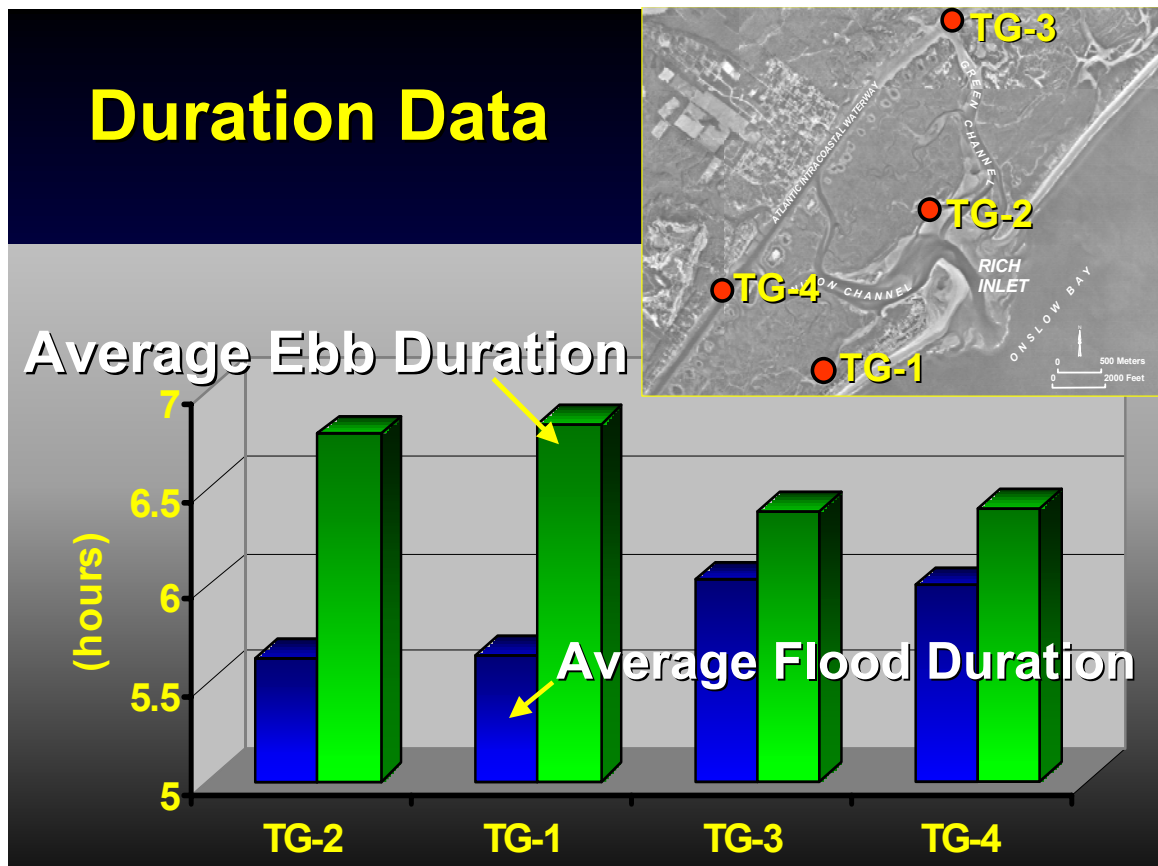


Figure 6. Average recorded flood (blue) and ebb (green) duration for each water-level meter.

Mean tidal lag times (in red), which were calculated between TG-2 and the other water-level meters are shown in Figure 5. Representative lag times were derived by averaging the high tide lag times calculated for each of the water-level meters for the study period. Lag times ranged from 0.1hrs at TG-4 (waterway south) to 0.58 hrs at TG-1 (tidal creek). The mean lag time recorded for TG-4 (waterway south) of 0.1 hrs was approximately 57% and 83% shorter than the tidal lag times recorded for TG-3 (waterway north) and TG-1 (tidal creek), respectively. The greater lag time at TG-3 (waterway north) compared to that recorded at TG-4 (waterway south), suggests that tidal flow was subjected to

increased levels of friction when propagating through the shoaled portions of Green Channel. This observation is consistent with the mean tidal range data, which showed a reduction in tidal amplitude between these stations. Further, the observed differences in lag times corroborate the contention that Nixon Channel is the dominant interior feeder channel.

ADCP Data

Channel Characteristics

ADCP data were collected along ten transects located throughout the interior channels and throat to characterize channel characteristics (Fig. 3). Channel surveys were conducted during varying tidal stage conditions. Survey data suggested a number of trends with respect to depth and shape of the channel network. Major morphologic differences were evident when comparing channel shape and cross-sectional area of Nixon and Green Channels. Transects 1, 3, and 4 (T-1, T-3, and T-4) located within Nixon Channel had a more hydraulically efficient channel shape due to a greater hydraulic radius (cross-sectional area/wetted perimeter as defined by MANNING, 1891) when compared to the channel segments at Transects 6, 7, and 8 (T-6, T-7, and T-8) located within Green Channel (Figs. 7 and 8). The average cross-sectional area of Nixon Channel was $\sim 893.4 \text{ m}^2$ ($9,616 \text{ ft}^2$), while the average depth at T-1, T-3, and T-4 on 8/6/2001 (conducted at high water) was 6.28 m (20.6 ft). It is important to note that channel depth and cross-sectional area were dependent

upon water level height. Tidal stage and corresponding depth, width, and A_c data for each survey are listed in Table 3.

Surveys conducted within Green Channel at T-6, T-7, and T-8 indicated that the mean maximum depth of the three channel transects was 4.3 m (14.11 ft), ~68% of the mean maximum depth (6.28 m [20.6 ft]) measured in Nixon Channel. When a comparison of the mean cross-sectional area from the major feeder channels was made, the results indicated that the mean channel cross-sectional area of Green Channel was ~ 44% (395.6 m^2 [4,258.7 ft^2]) of that measured in Nixon Channel (893.3 m^2 [9,615.7 ft^2]).

System Surveys										
2/14/2001 (began 0.5hrs after low water) – Tidal Range-1.01m										
Transect	T-1	T-2	T-3	T-4	T-5	T-6	T-7	T-8	T-9	T-10
Depth (m)	n/a	n/a	n/a	5.4	10.3	n/a	n/a	n/a	n/a	n/a
Width (m)	n/a	n/a	n/a	212.4	203.6	n/a	n/a	n/a	n/a	n/a
Area (m²)	n/a	n/a	n/a	661.8	1071.3	n/a	n/a	n/a	n/a	n/a
3/1/2001 (began 1.5hrs after high water) – Tidal Range-0.95m										
Transect	T-1	T-2	T-3	T-4	T-5	T-6	T-7	T-8	T-9	T-10
Depth (m)	5.9	2.9	6.2	n/a	10.9	4.2	3.4	5.3	5.1	5.6
Width (m)	197.8	67.5	253.2	n/a	220.5	137.3	145.2	132.1	164.2	158.2
Area (m²)	562.1	147.9	919.6	n/a	1175.7	386.2	365.0	554.2	458.1	468.6
6/19/2001 (began 2.5hrs after high water) – Tidal Range- 1.07m										
Transect	T-1	T-2	T-3	T-4	T-5	T-6	T-7	T-8	T-9	T-10
Depth (m)	4.9	2.7	6.6	5.6	12.1	3.0	2.7	5.2	5.3	5.0
Width (m)	140.0	62.3	209.7	280.1	237.5	130.6	114.6	101.1	148.9	204.9
Area (m²)	457.3	140.1	839.9	1156.1	1405.2	313.7	261.8	304.1	468.6	945.1
8/6/2001 (began at high water) – Tidal Range- 1.01m										
Transect	T-1	T-2	T-3	T-4	T-5	T-6	T-7	T-8	T-9	T-10
Depth (m)	5.6	3.0	7.1	6.2	12.3	3.8	3.2	5.9	5.5	5.5
Width (m)	135.1	72.3	215.1	295.6	264.8	175.4	107.6	138.3	124.5	173.2
Area (m²)	474.2	182.9	928.0	1277.8	1486.7	520.4	269.8	396.7	383.6	504.9

Table 3. Channel dimension data for ADCP surveys conducted within the inlet throat, primary feeder channels, and AIWW.

Surveys of the inlet throat (Transect 5) indicated that the mean inlet cross-sectional area ranged from 1,071.3 m² (11,531 ft²) on 2/14/01 to ~1,468.7 m² (16,003 ft²) on 8/6/01. Maximum throat depth ranged from 10.9 m (36 ft) on 2/14/01 to 12.2 m (40 ft) on 8/6/01. The maximum throat depth and cross-sectional area also were dependent upon survey water-level height. Tidal stage information is listed in Tables 1 and 3. Throat depth and cross-sectional area also varied slightly due to the presence of a scour hole located along the Hutaff Island shoulder immediately seaward of the flood ramp where Nixon Channel connects with the inlet throat. The shape and axis of the scour hole changed over the duration of the study period.

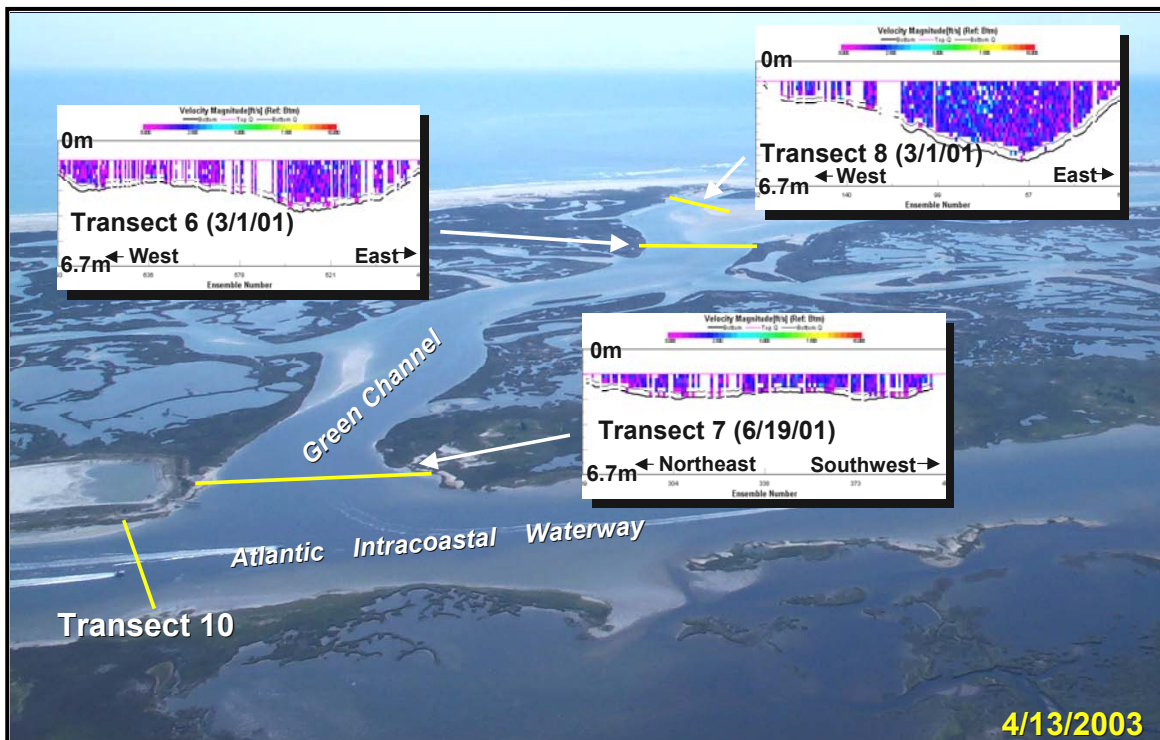


Figure 7. Oblique aerial photograph and ADCP generated channel cross-sections showing channel dimensions at Transects 6, 7, and 8 located within Green Channel.

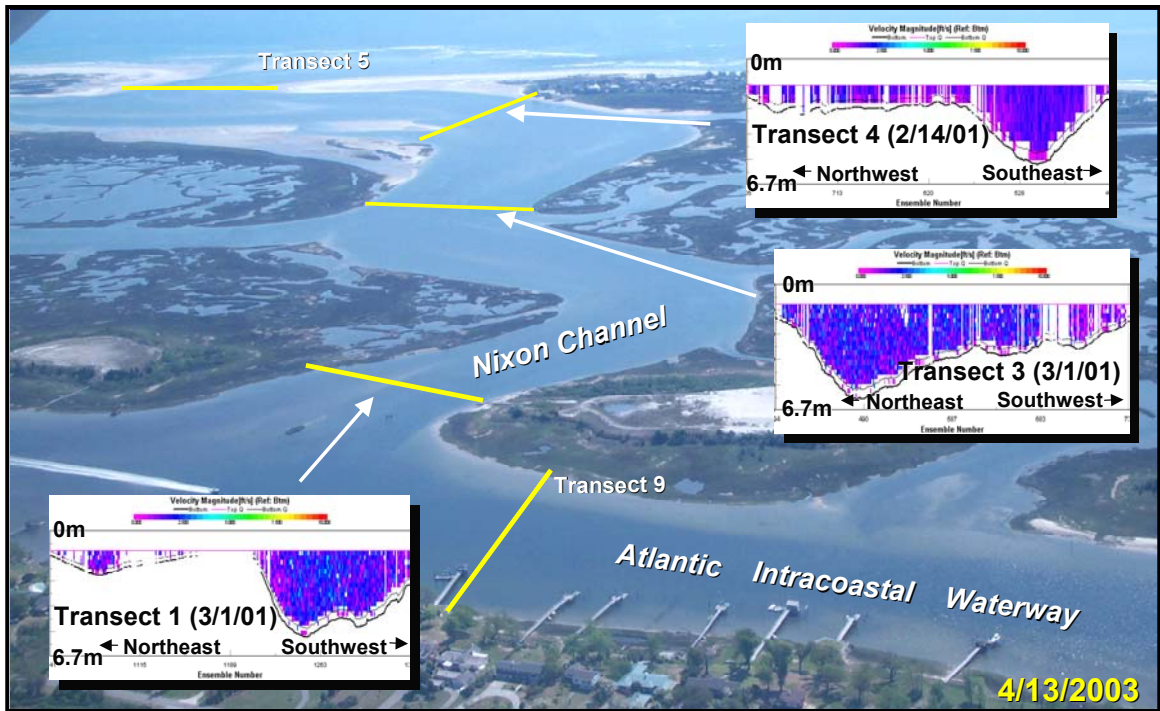


Figure 8. Oblique aerial photograph and ADCP generated channel cross-sections showing channel dimensions at Transects 1, 3, and 4 located within Nixon Channel.

Throat Surveys

A total of seven throat surveys were conducted along Transect 5 in order to accurately characterize inlet throat hydraulics (Fig. 9). Three throat surveys were conducted during the early phases of the study, where each survey was conducted over one-quarter of a tidal cycle (6 hr and 12.5 min) and provided preliminary hydrographic data (Table 4). The aforementioned surveys were conducted during portions of two spring ebb tides and one neap flood tide. Supplemental data were collected during four additional throat surveys (Tables 1, 4, and 5), which sampled one-half tidal cycles (12 hr and 25 min) during spring tides. A maximum spring flood velocity of 1.2 m/s (3.94 ft/s) and a maximum spring ebb velocity of 1.1 m/s (3.5 ft/s) were measured on 10/8/2002. The mean

spring flood and ebb velocity measured during the study period was 0.9 m/s (2.97 ft/s) and 0.84 m/s (2.75 ft/s), respectively. Compilation and inspection of the ADCP survey data indicated that the mean recorded spring flood duration was 5.76 hr. The mean recorded spring ebb duration of 6.6 hrs was 12.7% longer than the mean spring flood duration. ADCP duration data was consistent with the water-level data collected during the study period. The greater flood velocities and shorter flood durations documented during this study suggest that Rich Inlet is a flood dominant system (Fig. 10).



Figure 9. Oblique aerial photograph showing Rich Inlet throat and ADCP Transects 4, 5, and 8.

The average maximum spring ebb discharge was 1,054.0 m³/s (37,220 ft³/s), and the mean maximum spring flood discharge computed from ADCP data was 1,194.7 m³/s (42,193 ft³/s), or 12% greater than the ebb. Discharge data was used to calculate flood and ebb flow volumes for neap, average, and spring conditions. Calculated flow volume data indicated that spring ebb flow volumes

ranged from $12.17 \times 10^6 \text{ m}^3$ ($429.8 \times 10^6 \text{ ft}^3$) to $19.53 \times 10^6 \text{ m}^3$ ($689.73 \times 10^6 \text{ ft}^3$) with an average value of $15.91 \times 10^6 \text{ m}^3$ ($562 \times 10^6 \text{ ft}^3$). Measured spring flood volume ranged from $9.3 \times 10^6 \text{ m}^3$ ($329 \times 10^6 \text{ ft}^3$) to $22.58 \times 10^6 \text{ m}^3$ ($797.3 \times 10^6 \text{ ft}^3$), with a mean value of $17.08 \times 10^6 \text{ m}^3$ ($603 \times 10^6 \text{ ft}^3$).

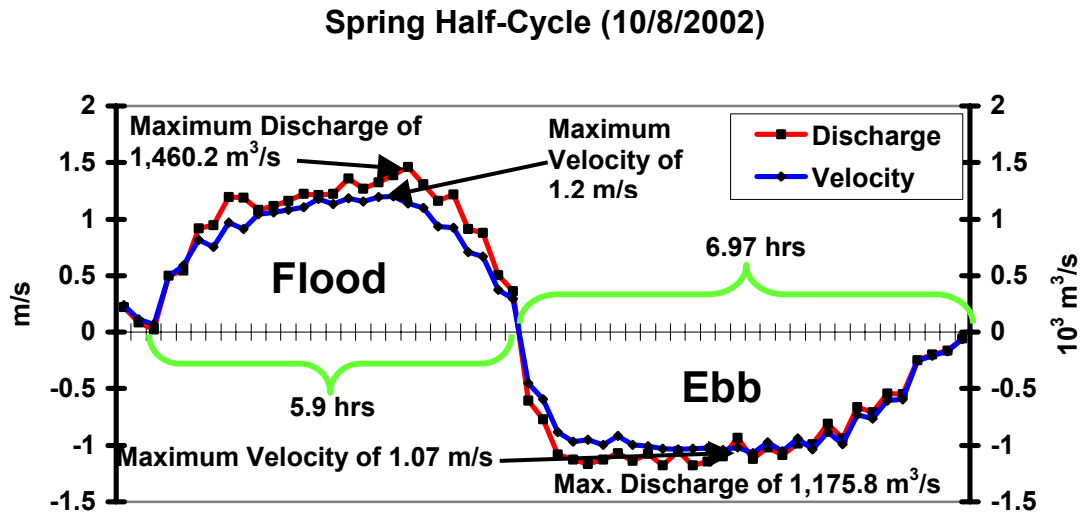


Figure 10. Velocity and discharge data showing the time-velocity asymmetry of Rich Inlet.

In order to measure the volume of water moving through Nixon Channel, and to establish its role as the primary feeder channel, a survey along Transect 4 was conducted concurrently with the throat survey conducted on 10/8/2002. Data from the Nixon Channel survey are listed in Table 5. The channel cross-sectional area at Transect 4, recorded during this survey, was $1,408 \text{ m}^2$ ($15,156 \text{ ft}^2$) and the maximum depth measured was 6.1 m (20 ft). Approximately 64% of the tidal prism (flood flow volume) and 68% of the ebb flow volume, measured at the inlet throat, were conveyed through Nixon Channel.

Rich Inlet Throat Parameters							
Survey Date	10/17/2001	11/30/2001	12/7/2001	1/16/2002		5/24/2002	
Tidal Setting	Spring Ebb	Spring Ebb	Neap Flood	Spring Ebb	Spring Flood	Spring Ebb	Spring Flood
Duration (hr)	6.77	6.5	5.67	6.22	6	6.63	6.07
Maximum Velocity (m/s)	0.808	0.902	0.805	0.698	0.515	0.866	0.954
Maximum Discharge (m ³ /s)	1,109.91	1,023.41	1,205.56	902.24	668.46	1,242.85	1,369.06
Volume (10 ⁶ m ³)	18.58	17.83	14.90	12.17	9.32	15.17	18.74
Channel Cross-sectional Area (m ²)	1,353.39	1,219.93	1,285.00	1,216.93		1,321.36	
Inlet Minimum Width (m)	273.55	271.23	261.93	277.23		228.1	
Depth (m)	8.98-11.13	8.84-11.11	9.36-11.08	9.2-10.63		8.68-11.21	
Predicted Range (m)	1.62	1.31	1.16	1.16	0.94	1.34	1.58
Observed Range (TG-2) (m)	1.43	1.31	1.13	1.1	0.85	1.31	1.62

26

Rich Inlet Throat Parameters					Nixon Channel	
Survey Date	7/24/2002		10/8/2002		10/8/2002	
Tidal Setting	Spring Ebb	Spring Flood	Spring Flood	Spring Ebb	Spring Flood	Spring Ebb
Duration (hr)	6.48	5.07	5.9	6.97	5.97	6.93
Maximum Velocity (m/s)	0.683	0.951	1.201	1.067	0.668	0.622
Maximum Discharge (m ³ /s)	869.47	1281.36	1460.21	1175.82	950.66	820.46
Volume (10 ⁶ m ³)	12.20	17.70	22.58	19.53	14.40	13.26
Channel Cross-sectional Area (m ²)	1,237.99		1,133.14		1,408.08	
Inlet Minimum Width (m)	222.25		197.22		N/A	
Depth (m)	8.95-10.9		8.44-10.7		4.03-6.1	
Predicted Range (m)	1.1	1.4	1.68	1.62	1.68	1.62
Observed Range (TG-2) (m)	1.07	1.34	1.68	1.52	1.68	1.52

Tables 4 and 5. ADCP and tide range data for each of the seven throat surveys. Table 5 also contains data collected during the Nixon Channel survey conducted on 10/8/2002.

The flood flow duration of 5.97 hr recorded within Nixon Channel on 10/8/2002 was slightly greater than the flood flow duration of 5.90 hr recorded at the throat during the same survey period. The recorded maximum flood velocity at Transect 4 was 0.67 m/s (2.19 ft/s) while the recorded maximum ebb velocity was ~7% less (0.62 m/s [2.04 ft/s]). The maximum velocity (0.67 m/s [2.19 ft/s]) recorded during the flood portion of the tidal cycle was ~55.6% of the mean maximum velocity (1.20 m/s [3.94 ft/s]) recorded at the inlet throat. The maximum ebb current velocity was slightly slower (0.62 m/s [2.04 ft/s]) and was 58.3% of the velocity measured (1.07 m/s [3.5 ft/s]) at the inlet throat. The maximum flood discharge at Transect 4 in Nixon Channel was ~65% (~950.7 m³/s [33,572 ft³/s]) of that measured at the inlet throat whereas the maximum ebb discharge was ~69.8% (820.5 m³/s [28,974 ft³/s]). The recorded ebb volume was ~8% less (13.25 x 10⁶ m³ [468 x 10⁶ ft³]) than the recorded flood volume of 14.38 x 10⁶ m³ (508 x 10⁶ ft³).

As a result of appreciable variations in tidal amplitude during each of the seven throat surveys (Tables 4 and 5), tidal prisms, velocities, and durations varied considerably. Measured tidal ranges and tidal prisms for each of the seven throat surveys are listed in Tables 4 and 5. Inequalities in flood and ebb discharge values were due primarily to tidal amplitude inequality associated with the timing of each survey.

Tidal Range Influence on Flow Parameters

Tidal Range versus Flow Volume

The range of values for the measured inlet hydraulic parameters appeared to be related to the varying effects of tidal range. Figure 11 depicts relationships between ebb/flood tidal range and associated flow volumes. To identify a predictable relationship between tidal range and tidal prism, flow volumes were regressed against tidal range for each survey date. Tidal prisms for flood and ebb flows were regressed against tidal range for each survey date. Both the flood and ebb flow volumes were significantly and positively related to the tidal range.

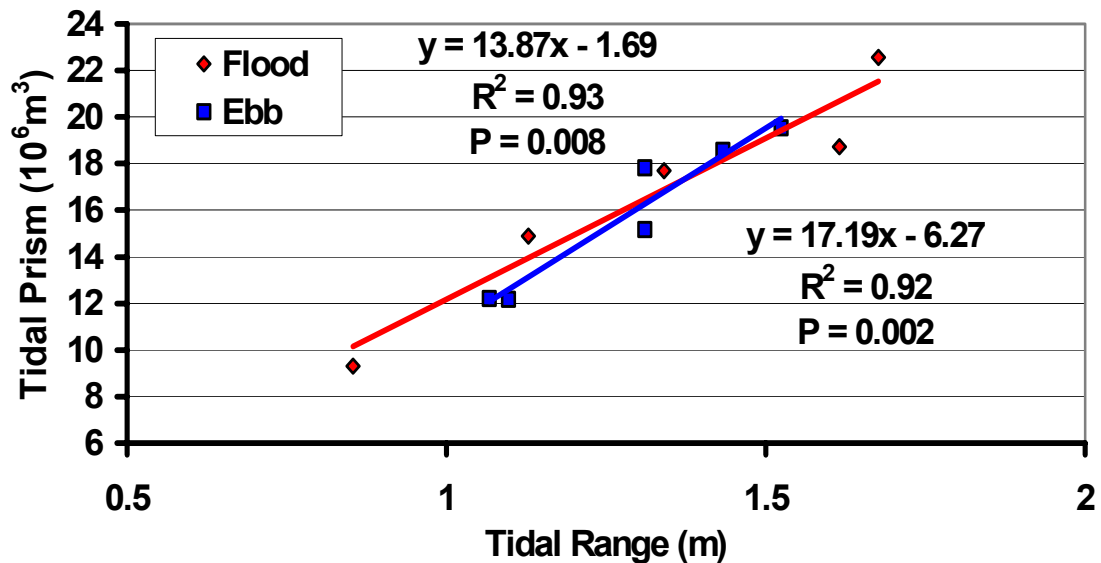


Figure 11. Relationship between measured tidal range and flood/ebb flow volumes.

In order to accurately predict flow volumes during neap, average, and spring conditions, the predicted flood and ebb flow volumes were calculated using the derived regression equations and the mean recorded tidal range at TG-

2 (1.08 m [3.54 ft]). The resulting volumes were $13.27 \times 10^6 \text{ m}^3$ ($468.5 \times 10^6 \text{ ft}^3$) and $12.28 \times 10^6 \text{ m}^3$ ($433.7 \times 10^6 \text{ ft}^3$), respectively. Based on these predictions, the flood flow volume ($9.0 \times 10^6 \text{ m}^3$ [$317.7 \times 10^6 \text{ ft}^3$]) should decrease by 32% during neap tide conditions ($t_r = 0.77 \text{ m}$ [2.53 ft]). The predicted ebb flow volume ($6.99 \times 10^6 \text{ m}^3$ [$246.8 \times 10^6 \text{ ft}^3$]) should decrease by 43%. The calculated differences were relative to the predicted mean flow volumes identified previously. For an average spring tidal range of 1.44 m (4.72 ft), the flood and ebb flow volumes predicted by the linear regression model were $18.25 \times 10^6 \text{ m}^3$ ($644.6 \times 10^6 \text{ ft}^3$) and $18.46 \times 10^6 \text{ m}^3$ ($652 \times 10^6 \text{ ft}^3$), respectively. The predicted spring flood ($\sim 18.25 \times 10^6 \text{ m}^3$ [$644.6 \times 10^6 \text{ ft}^3$]) and ebb ($18.46 \times 10^6 \text{ m}^3$ [$652 \times 10^6 \text{ ft}^3$]) volumes differed by about 1%.

During mean tidal conditions ($t_r = 1.08 \text{ m}$ [3.54 ft]) and neap tidal conditions ($t_r = 0.77 \text{ m}$ [2.53 ft]), the flood flow volume is typically greater than the ebb flow volume. During spring tidal conditions ($t_r = 1.44 \text{ m}$ [4.72 ft]), however, the ebb flow volume exceeds the flood flow volume. Using yearly tidal data for the study area, flood flow volumes should exceed ebb flow volumes 87% of the time. In general, the bias towards a larger predicted flood flow decreased with increasing tidal range. This trend continues until predicted flood and ebb flow volumes are equal at a tidal range of 1.37 m (4.51 ft). Once the tidal range exceeds 1.37 m (4.51 ft), the ebb flow volume exceeds the flood flow volume, suggesting that the system begins to display an ebb-bias. However, as mentioned previously, during spring conditions the flood and ebb volumes varied by only about 1%, with a greater ebb volume. The predicted difference between

the flood and ebb volumes is ~22% during neap conditions with a greater predicted flood flow volume.

Tidal Range versus Velocity

Tidal range at TG-2 and the maximum current velocity measured during individual surveys at the throat were significantly and positively correlated (Fig. 12). The linear model produced by the regression analysis was used to calculate max flood and ebb velocities for a mean recorded tidal range of 1.08 m (3.54 ft) (TG-2). The predicted maximum flood and ebb current velocities (under normal conditions) were calculated to be 0.72 m/s (2.35 ft/s) and 0.69 m/s (2.27 ft/s). This method predicted an increase in maximum current velocities of 26% for both the flood and ebb currents during spring tide conditions ($tr = 1.37$ m [4.72 ft]), with a predicted maximum flood velocity of 0.97 m/s (3.17 ft/s) and a predicted maximum ebb current velocity of 0.94 m/s (3.08 ft/s). During neap conditions, the predicted flood velocity decreased to 0.50 m/s (1.66 ft/s) whereas maximum ebb velocities decreased to 0.48 m/s (1.57 ft/s). It is important to note that maximum flood velocities are expected to exceed maximum ebb velocities through the entire range of normal tidal conditions.

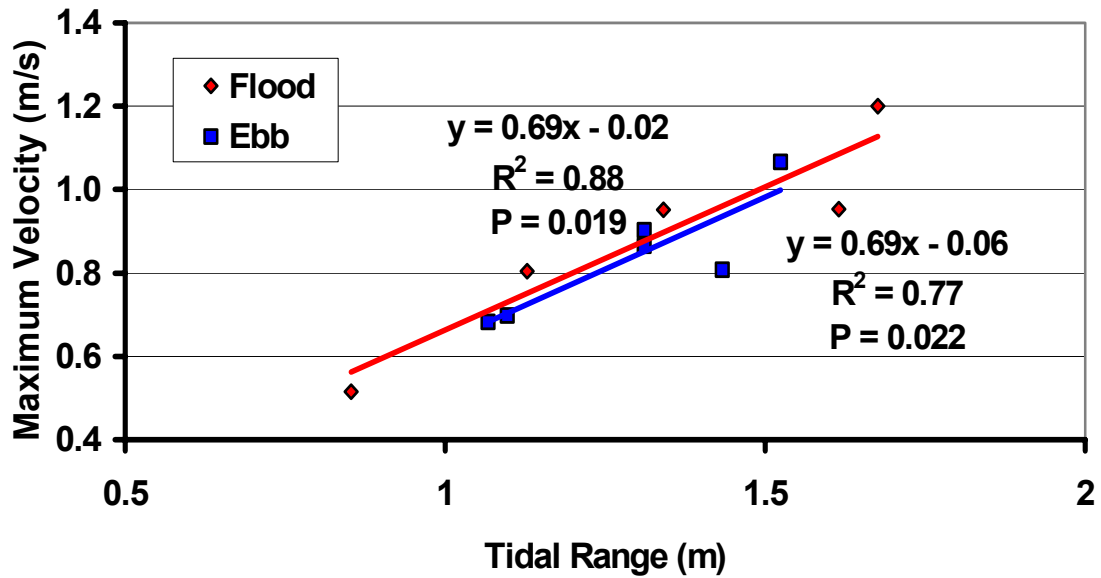


Figure 12. Relationship between measured tidal range and flood/ebb maximum velocities.

Tidal Range versus Discharge

The relationship between measured flood and ebb discharge and tidal range was slightly weaker than the relationship between tidal range and velocity or tidal prism. The relationships between tidal range and recorded ebb and flood discharge volumes are shown in Fig 13. Using the average recorded tidal range of 1.08 m (3.54 ft), the resulting mean predicted flood and ebb discharge were 993.6 m³/s (35,089 ft³/s) and 911.0 m³/s (32,172 ft³/s), respectively. Predicted discharge values were 1,293.5 m³/s (45,680 ft³/s) for the flood and 1,154.3 m³/s (40,762.86 ft³/s) for the ebb during spring conditions; increases above the mean values were 23% and 21%, respectively. Under neap conditions, predicted flood and ebb discharge values decreased from the mean values by 26% (736.9 m³/s [26,023 ft³/s]) and 23% (702.8 m³/s [24,819 ft³/s]), respectively.

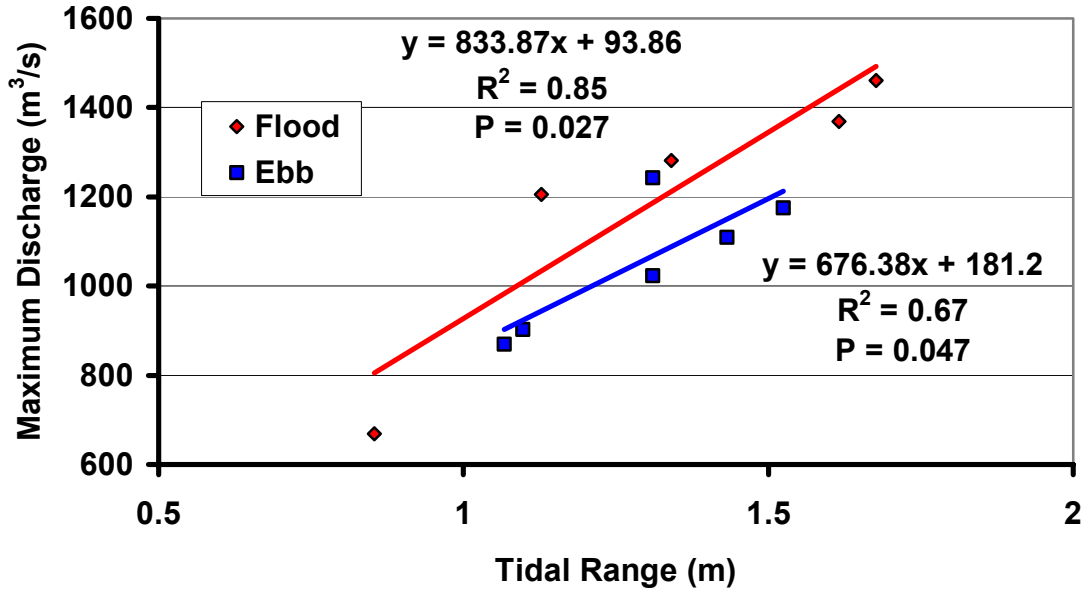


Figure 13. Linear regression plot depicting relationship between measured tidal range and flood/ebb discharge.

Tidal Prism

Previous investigations have utilized a variety of tidal prism definitions (ATM, 1999; MCNINCH, 2003; MILITELLO and KRAUS, 2001; WSE, 2001). The majority of these definitions have identified tidal prism as the volume of water, excluding freshwater, that flows in or out of an estuary or bay with the movement of the tide (BATES and JACKSON, 1995). Other studies focused on inlet hydraulics have identified tidal prism as the volume of water that is drawn into a bay from the ocean through the inlet during a flood tide (SEABERGH, 2003). In order to characterize near maximum magnitudes, tidal prism for purposes of this study is defined as the volume of water that enters an inlet on a spring flood tide. The “measured” tidal prism values during this investigation were calculated from discharge data obtained during ADCP surveys. Tidal prism values were variable,

ranging from $9.32 \times 10^6 \text{ m}^3$ ($329 \times 10^6 \text{ ft}^3$) to $22.57 \times 10^6 \text{ m}^3$ ($797 \times 10^6 \text{ ft}^3$) (Tables 4 and 5). The mean “measured” T_p for the study period was $17.1 \times 10^6 \text{ m}^3$ ($603 \times 10^6 \text{ ft}^3$). Variations in the values of tidal prism were directly related to differences in the tidal ranges during individual surveys. The relationship between tidal range and flood flow volume is given by the regression equation (Fig. 11):

$$FV = 1.387 \times 10 (r) - 1.69 \quad (1)$$

Where FV = flow volume (10^6 m^3) and r = tidal range (m). Using Equation 1 and the mean recorded spring tidal range of 1.44 m (4.72 ft) (TG-2), the predicted tidal prism was determined to be $18.25 \times 10^6 \text{ m}^3$ ($645 \times 10^6 \text{ ft}^3$). It is important to note that the empirically derived T_p value of $18.25 \times 10^6 \text{ m}^3$ ($645 \times 10^6 \text{ ft}^3$) is only 6.5% greater than the mean measured T_p of $17.1 \times 10^6 \text{ m}^3$ ($603 \times 10^6 \text{ ft}^3$).

Flow data from an ADCP survey conducted on 7/23/99 by ATM (1999) for the Mason Inlet EIS was used in conjunction with Equation 1 in order to examine differences between the predicted and measured tidal prism values. The ATM survey recorded a flood flow volume of $\sim 9.21 \times 10^6 \text{ m}^3$ ($325 \times 10^6 \text{ ft}^3$) (1999). The aforementioned survey was conducted five days prior to a spring tide with a predicted range of 1.06 m (3.47 ft). In accordance with the relationship established by Equation 1, a tidal range of 1.06 m (3.47 ft) would yield a tidal prism value of $\sim 12.97 \times 10^6 \text{ m}^3$ ($458 \times 10^6 \text{ ft}^3$). The resulting predicted T_p value was approximately 29% larger than the measured value derived from the ATM

survey. Differences between the predicted and observed tidal prism are most likely attributable to the influence of environmental conditions including wind and possibly freshwater input.

Numerous studies have shown that there is a direct relationship between the inlet throat cross-sectional flow area and the calculated tidal prism (JARRETT, 1976; NAYAK, 1971; O'BRIEN, 1969). A comparison of values for the mean measured tidal prism and the calculated tidal prism was made utilizing the widely used regression equation of Jarrett (1976) (Equation 2).

$$A_c = 3.039 \times 10^{-5} P^{1.05} \quad (2)$$

In the equation above, A_c = inlet cross-sectional area (m^2) and P = tidal prism (m^3). The value for the cross-sectional area used in Jarrett's equation represented the mean of the median cross-sectional area value ($A_c = 1,227 m^2$ [13,211 ft^2]) measured during each of the four throat surveys conducted during spring flood tide conditions (Table 4 and 5). The resulting calculated tidal prism, based on Equation 2, was $17.5 \times 10^6 m^3$ ($619.5 \times 10^6 ft^3$). The difference between the calculated T_p ($17.5 \times 10^6 m^3$ [$619.5 \times 10^6 ft^3$]) and the mean measured tidal prism ($17.1 \times 10^6 m^3$ [$603.3 \times 10^6 ft^3$]) was ~3%. The calculated T_p of $17.5 \times 10^6 m^3$ ($619.5 \times 10^6 ft^3$) from Equation 2, is about 4% less than the T_p value of $18.25 \times 10^6 m^3$ ($644.56 \times 10^6 ft^3$) empirically derived during this study. The difference between the two approaches and the measured T_p value suggest that the

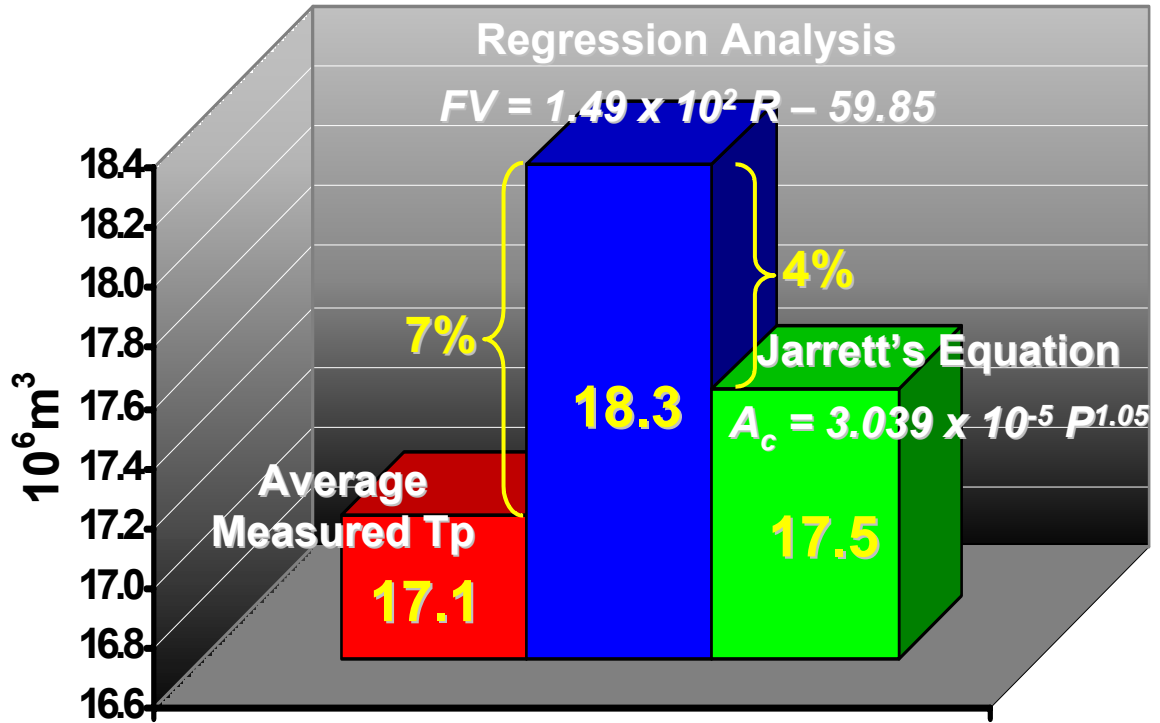


Figure 14. Differences in derived tidal prism values relative to directly measured values.

values generated in this study are accurate. Considering that the majority of surveys were conducted on days with below-average spring tidal ranges, a realistic T_p value for this inlet most likely lies between $17.5 \times 10^6 \text{ m}^3$ ($619.5 \times 10^6 \text{ ft}^3$) and $18.25 \times 10^6 \text{ m}^3$ ($644.56 \times 10^6 \text{ ft}^3$).

Analyses of the A_c values from individual throat surveys (Tables 3-5) yielded tidal prism values that ranged from $16.3 \times 10^6 \text{ m}^3$ ($574 \times 10^6 \text{ ft}^3$) to $18.8 \times 10^6 \text{ m}^3$ ($664 \times 10^6 \text{ ft}^3$). The differences between the predicted T_p , using Equation 2, and “measured” T_p ranged from 1% to 47%. Presumably, the aforementioned differences are attributable to variations in tidal amplitude during the surveys.

A comparison of the predicted and measured A_c values and their relationships to the mean of the measured T_p values ($17.08 \times 10^6 \text{ m}^3$ [603×10^6

ft³) was also conducted using Equation 2. These calculations yielded a value for A_c of 1,193.56 m² (12,847 ft²), ~5% less than the average measured A_c of 1,252 m² (13,482 ft²). Using the T_p value of 18.25×10^6 m³ (644.56×10^6 ft³) derived from the regression analysis, the cross-sectional flow area would have been 1,279.6 m² (13,773 ft²). This value is only ~2% greater than the mean measured A_c of 1,252.54 m² (13,482.23 ft²). The strong agreement between predicted and measured A_c values suggests, again, that the survey data are highly accurate.

Ebb-Tidal Delta Retention Capacity

In order to estimate the volume of sediment retained in the ebb-tidal delta, the derived T_p values were used in conjunction with WALTON and ADAMS' (1976) equation. The volume of sediment retained in the outer bar (ebb-tidal delta) is primarily a function of tidal prism and local wave climate (WALTON and ADAMS, 1976). This relationship is expressed by the equation:

$$V = 13.8 \times 10^{-5} T_p^{1.23} \quad (3)$$

where V = outer bar volume (yd³) and T_p = tidal prism (ft³). Calculations of volume using the tidal prism value derived from the regression analysis (18.26×10^6 m³ [645×10^6 ft³]) resulted in an ebb-tidal delta volume of 7.23×10^6 m³ (9.45×10^6 yd³). The resulting value of the ebb-tidal delta volume using Equation 3 decreased to 6.87×10^6 m³ (8.99×10^6 yd³) when the T_p (17.53×10^6 m³ [619×10^6 ft³]) derived from Equation 2 was used. The predicted ebb-tidal delta volume

decreased further to $6.66 \times 10^6 \text{ m}^3$ ($8.71 \times 10^6 \text{ yd}^3$) when calculations were based on the mean measured T_p of $17.08 \times 10^6 \text{ m}^3$ ($603 \times 10^6 \text{ ft}^3$). Rich Inlet ebb shoal volumes are relatively large when compared to those determined for nearby Carolina Beach ($5.6 \times 10^6 \text{ m}^3$ [$7.3 \times 10^6 \text{ yd}^3$]) and Mason ($1.8 \times 10^6 \text{ m}^3$ [$1.8 \times 10^6 \text{ yd}^3$]) Inlets (WELSH, 2003; USACE, 2003). The precise volume of the sand contained in the ebb-tidal delta (outer bar) is difficult to assess and can only be accurately determined by detailed bathymetric surveys. Regardless, the above data do provide estimates of the outer bar volume, which are important for future management considerations. The data associated with the predicted ebb-tidal delta volumes are useful for establishing baseline information for future investigations of the inlet.

Variations in the volume of ebb-tidal deltas of selected Florida inlets was examined by MARINO and MEHTA (1987), who emphasized the importance of the inlet aspect ratio (W/D) and its relationship to the volume of sediment contained in the ebb-tidal delta. Their findings suggested that two inlets could have similar cross-sectional areas but have vastly different W/D ratios. Furthermore, results from their investigation indicated that as the inlet aspect ratio decreases, the ebb tidal delta volume increased, emphasizing the importance of throat channel shape and its influence on the ebb-tidal delta volume.

The current study determined that Rich Inlet had a mean aspect ratio of 22.56. The range of the inlet aspect ratios was small (18.43 to 26.09). The lesser value indicated a narrower, deeper channel shape; the greater value

indicated a wider, shallower channel cross-section. Generally, inlet aspect ratios decreased over the duration of the study, indicating that the throat had narrowed and deepened slightly, thus increasing the volume of material retained in the ebb-tidal delta. It is highly unlikely that the volume of material in the outer bar changed as rapidly as the shape of the inlet throat during this study, however due to the lack of detailed bathymetry throughout the ebb shoal this assumption cannot be confirmed. Nonetheless, the data derived from MARINO and MEHTA (1987) indicate that major differences in the aspect ratio will likely play a role in the volume of sand contained in the offshore shoals.

Channel Sediments

Standard sedimentological analyses of the 97 samples indicated the sediments ranged from silty-sand near the cut bank margins to coarse gravels (shell gravels) within the thalwegs. The majority of the coarsest sediments were located within the inlet throat and thalwegs of Nixon and Green Channels. Coarse shell hash, and gravel size shell fragments formed an armor or shell pavement along portions of the channel segments where flow velocities were highest. The floor of the inlet throat was characterized by the presence of mega-ripples comprised of coarse shell hash, ranging in size from coarse sand to gravel fragments of lithoclasts and shell debris.

Samples containing higher percentages of fine material were usually found within the landward reaches of the channel system, particularly near the AIWW (Transects 1, 7, 9, and 10), and along the cut bank margins of the larger

channels. Samples collected along Transects 4, 5, and 8 contained only trace amounts of fine material. Occasionally large shell fragments were found in samples collected on the channel slopes fronting the cut bank margins. The percentage of carbonate material (shell material) was highly variable and ranged from less than 5% to more than 60%. Increased grain size was usually correlated with increased carbonate content (shell). Folk and Ward's (1957) classification was used in determining textural groups and statistics. The samples ranged from sandy gravels to sand (Tables 1-3, Appendix). Approximately 52% of the samples were classified as slightly gravelly sands.

DISCUSSION

Information pertaining to inlet throat dimensions, obtained from ADCP surveys, indicated that throat morphology underwent significant change during the course of the study. The average inlet width during the study period was 247 m (811 ft) and ranged from 197 – 277 m (647 – 909 ft). The maximum depth within the inlet throat also varied, and ranged from approximately 10.7 – 11.3 m (35 – 37 ft). Consequently, inlet cross-sectional area varied during the course of the study. The mean throat cross-sectional area was 1,252.5 m² (13,482 ft²), with values ranging from 1,133.1 to 1,353.4 m² (12,197 – 14,568 ft²). Changes in throat morphology were ultimately due to variations in the alignment of the ebb channel and associated shoulder adjustments. These variations may have had appreciable impacts on inlet hydraulics.

ADCP data collected within Nixon and Green Channels indicated a number of general trends related to interior channel shape. Nixon Channel appeared to be the dominant feeder channel, with a more hydraulically efficient channel shape (semi-circular) with greater hydraulic radius and depth when compared to that of Green Channel (MANNING, 1891). Survey data collected within Green Channel indicated that the average maximum depth was approximately 68% of the average maximum depth of Nixon Channel. Accordingly, data indicated that the average channel cross-sectional area of Nixon Channel ($\sim 893.4 \text{ m}^2$ [9616 ft^2]) was approximately 45% larger than that of Green Channel (395.6 m^2 [4,258.7 ft^2]).

Flow data obtained through ADCP throat surveys provided important information concerning velocity and discharge. These data were incorporated into a number of regression models in order to accurately predict flow velocity, discharge, and volume under a variety of tidal conditions. Information obtained from these regression models indicated a number of important trends associated with changes in flow during neap, normal, and spring conditions. Discharge and velocity data both indicated a flood bias with greater values predicted for the flood portion of the tide under all tidal conditions. Flood bias was also evident in portions of the flow volume regression model. However, bias was not consistent over the entire range of tidal conditions. It was determined that the flood flow volume, under most conditions, was greater than the ebb flow volume. However this trend weakened with increasing tidal range, until the two volumes were predicted to be equal at a tidal range of 1.37 m (4.51 ft). During spring conditions

(1.44 m [4.72 ft]), it was determined that the ebb flow volume exceeded the flood flow volume by approximately 1%. Reasons for this apparent shift in flow volume bias is most likely attributable to error associated with the conversion of discharge data to volume. However, it is possible that these apparent trends are real, which would indicate a shift in regional flow patterns with differing tidal amplitudes.

Disparities between flood and ebb flow volumes have been recorded in a number of other hydrographic investigations within tidal inlets (MITELLO and KRAUS, 2001; WSE, 2001). Inequalities have been attributed to differences between flood and ebb amplitudes and water level being out of phase with the tidal current. Flood and ebb flow volume disparities, in marsh-filled, multiple-inlet systems, are extremely difficult to identify and may be caused by variables such as changing wind conditions and the influence of freshwater input. These variables coupled with complex lagoonal circulation patterns make understanding changes in flow volume a difficult task. The focus of this study was aimed at identifying and characterizing the hydrographic parameters present within Rich Inlet and associated primary feeder channels. Future work within the area should involve the conduct of similar hydrographic investigations for neighboring inlets and AIWW in order to address the identification of circulation patterns on a regional basis.

Tidal prism (T_p) data were generated by converting the measured discharge data recorded during ADCP surveys. The measured tidal prism data set was supplemented with a variety of T_p values utilizing several different

empirical methods. The measured T_p was derived by averaging the values from each of the four throat surveys conducted during spring flood tide conditions, resulting in a T_p value of $17.08 \times 10^6 \text{ m}^3$ ($603.27 \times 10^6 \text{ ft}^3$). The second T_p estimation was derived from a regression analysis equation (1) relating tidal prism to tidal range. The resulting T_p , using Equation 1 and the average measured spring tidal range at the inlet throat (1.43 m [4.72 ft]), was $18.25 \times 10^6 \text{ m}^3$ ($644.56 \times 10^6 \text{ ft}^3$). An additional estimate of the inlet T_p ($17.53 \times 10^6 \text{ m}^3$ [$619 \times 10^6 \text{ ft}^3$]) was made using Jarrett's equation (Equation 2) and the average measured A_c of $1,227.35 \text{ m}^2$ ($13,211 \text{ ft}^2$). These values are relatively large when compared to the tidal prisms determined for other inlets located within the Onslow Bay of North Carolina. For example, nearby Mason and Carolina Beach Inlets are estimated to have tidal prisms of $5 \times 10^5 \text{ m}^3$ ($169 \times 10^6 \text{ ft}^3$) and $15 \times 10^6 \text{ m}^3$ ($525 \times 10^6 \text{ ft}^3$), respectively (WELSH, 2003; USACE, 2003). Larger inlets such as Cape Fear, Masonboro, and Beaufort Inlets do exist within the region; however, these systems are artificially stabilized through the implementation of hard structures or active dredging, therefore making it difficult to assess what would be their natural flow conditions.

Water-level data coupled with the discharge and current velocity data collected from the throat showed that Rich Inlet is a flood dominant system. Flood dominance was indicated by greater maximum velocities during the flood portion of the cycle as opposed to the slower velocities measured during ebb flow. Maximum discharge was also greater during flood flow rather than the ebb portion of the cycle. The maximum flood velocities recorded were greater than

the ebb velocities for most of the surveys. Discharge and velocity data derived during this study agree well with data recorded at nearby Mason Inlet where maximum flood velocities and discharge typically exceeded ebb velocities and discharge (WELSH, 2003). Flood dominance was also indicated upon inspection of flow data from the Nixon Channel survey and showed that the maximum recorded flood flow velocity (0.67 m/s [2.19 ft/s]) was approximately 0.04 m/s (0.15 ft/s) faster than the ebb current velocity (0.62 m/s [2.03 ft/s]). Flood and ebb flow maximum velocities were approximately 44% of the maximum flow velocities recorded at the inlet throat on the same day. Decreases in flow velocities are expected due to increased friction associated with Nixon Channel dimensions. Discharge data reinforced a strong flood bias within the feeder channel. An analysis of the flow data indicated that approximately 64% of the tidal prism (spring flood flow volume) and 68% of the ebb flow volume was conveyed through Nixon Channel. Nixon Channel dominance may play an important role in controlling the inlet throat location. An ongoing study by JACKSON (2003), based on analysis of aerial photographs dating from 1938 to 2003, indicates that the Rich Inlet throat has generally migrated north over the past three years and reached its most northerly position in March, 2003. Northerly migration may have been related to the greater flow volume moving through Nixon Channel and subsequent shoaling of Green Channel. Future work involving the synthesis of the JACKSON (2003) database and that of this study will seek to identify the inter-relationships between inlet flow patterns and inlet morphology.

Inlet flood dominance is further corroborated by flood and ebb flow duration data derived from the water-level meters and ADCP surveys. Throat survey (ADCP) data showed that the average flood current duration (5.63 hr) was 1.15 hours shorter than the average ebb current duration (6.78 hr). Assuming that near equal flood and ebb flow volumes exist, shorter flood durations indicate greater flood flow velocities. Flood flow durations were consistently less than ebb flow durations during all throat surveys (Tables 4 and 5). Inspection of the water-level data obtained from an instrument located near the inlet throat (TG-2) was consistent with the data obtained during the ADCP surveys. Flood flow dominance weakened with distance from the throat, resulting in significantly less difference between the flood and ebb current durations. The average flood current duration in the landward reaches of Green Channel near the AIWW was 6.03 hr whereas the ebb current duration (6.38 hr) was 0.35 hr longer, correspondingly the average flood duration was only ~5% less than the recorded average ebb flow duration. Similar flood and ebb flow durations were recorded in the landward portion of Nixon Channel. Increases in flood flow durations and decreases in ebb flow durations with distance from the inlet throat are most likely attributable to influence of the AIWW.

Due to the lack of detailed hydrographic investigations within the area, it cannot reasonably be determined whether flood dominance is typical for similar lower-mesotidal mixed-energy tidal inlets within North Carolina. Early work based on overall inlet morphology suggests that the majority of inlets within the area may be flood dominant due to the presence of well-defined flood tidal deltas

(Hayes, 1994). Data derived as part of an ongoing study by WELSH (2003) reinforces this contention and suggests that nearby Mason Inlet is flood dominant. A study by Seelig and Sorenson (1978) found that an ocean tidal asymmetry typical for many east coast locations with semidiurnal tides, favored flood dominance within tidal inlets, coincidentally the location used in the study was Wilmington, NC. Flood dominance has also been documented at many tidal inlets along other portions of the eastern U.S. (AUBREY and SPEER, 1985; LINCOLN and FITZGERALD, 1988; MOTA OLIVEIRA, 1970; USACE, 2003; ZARILLO and MILITELLO, 1999).

Explanation of flood dominance was previously examined in studies by BOON III and BYRNE (1981) and FITZGERALD and NUMMEDAL (1983) which documented that inlets with large open bays tend to exhibit flood dominated currents and conversely, inlets with bays containing variable areas, including marsh and small channels, tend to exhibit ebb dominant currents. Other studies have determined that open bays or bays filled with supratidal marsh tend to display flood dominant currents (MOTA OLIVEIRA, 1970; AUBREY and SPEER, 1985). Flood current dominance within Nauset Inlet, Massachusetts was previously examined by AUBREY and SPEER (1985), who attributed flood dominance to a lack of non-linear basin filling associated with channel friction related to the presence of high marsh (supratidal). Other explanations of flood tide dominance include tidal truncation, which occurs when the ocean tide level falls below the minimum channel depths within the inlet (LINCOLN and FITZGERALD, 1988). Although numerous explanations concerning flood tide

dominance exist, “a complete physical explanation for these tendencies is yet to be put forward” (DILORENZO, 1988). Similarly, an explanation of flood tide dominance within the Rich Inlet system has yet to be determined.

Sedimentological data indicated that Rich Inlet and associated feeder channels is dominated by relatively coarse sediments. These sediments are indicative of a high-energy environment with swift currents. Rich Inlet and the primary feeder channels are most likely infilling with sediment due to the flood dominance indicated by the collected current and flow duration data. Sediment composition and grain size existing within the inlet and feeder channels closely matched that of the material found within the ebb-tidal delta and adjacent beaches. System infilling is reinforced by observations made concerning a dredged area located within Nixon Channel. During the course of the study, a portion of the flood shoal previously removed in early 2001 for navigation improvements was completely recharged with relatively clean fine to medium grained sand. The material was consistent with the material found on the present day beach and ebb-tidal delta. Long-term implications of system infilling will most likely result in a reduction of tidal prism, possibly altering inlet stability.

CONCLUSIONS

The data obtained throughout the course of this investigation has provided a detailed baseline of hydrographic and sedimentological parameters. Major findings of this study include:

1. Rich Inlet system is relatively large compared to the majority of tidal inlets in North Carolina. Tidal prism was determined to be approximately $18.3 \times 10^6 \text{ m}^3$, which resulted in an estimated ebb-tidal delta retention capacity of approximately $7.23 \times 10^6 \text{ m}^3$.
2. Rich Inlet is a flood dominant system, indicated by greater flood velocities and shorter flood durations.
3. Nixon Channel is the dominant feeder channel. Indicated by greater depth and more efficient channel shape. Handles ~66% of the flow moving through the inlet.
4. Sediments are primarily composed of medium sand and shell gravel.

Future inlet modification related to navigation, water quality, or nourishment-related dredging activities may have significant impacts upon the bias of the inlet system and its sand bodies. Alteration may lead to an increased tidal prism and an increase in the size of the ebb-tidal delta. Changes in the extent and volume of the ebb-tidal delta will manifest itself in erosion of one or both of the adjacent shoulders and oceanfront shorelines. This investigation provides a detailed framework for future studies associated with modification of the inlet system and as a comparative template for other inlet studies. The ability to predict and identify the potential impacts associated with system modifications will drastically reduce the cost to both the environment and local municipalities.

LITERATURE CITED

- APPLIED TECHNOLOGY AND MANAGEMENT (ATM) of North Carolina, 1999. *Environmental Assessment: Mason Inlet Relocation Project*. Wilmington, NC.
- AUBREY, D.G. and SPEER, P.E., 1985. A Study of Non-Linear Tidal Propagation in Shallow Inlet/Estuarine Systems. Part I: observations. *Estuarine Coastal Shelf Science*, v.21, pp. 185-205.
- BAKER, S., 1977. *The Citizen Guide to North Carolina's Shifting Inlets*, North Carolina Sea Grant Program, SG-77-08. North Carolina State University, Raleigh, NC. 32p.
- BATES, R.L. and JACKSON, J.A., 1995. *Glossary of Geology CD-ROM*, Third Edition. American Geological Institute, Alexandria, VA.
- BLOTT, S.J. and PYE, K., 2001. *Gradistat: A Grain Size Distribution and Statistics Package for the Analysis of Unconsolidated Sediments*. Surface Processes and Modern Environments Research Group, University of London. John Willey and Sons, Ltd, p. 1-12.
- BOON III, J.D. and BYRNE, R.J., 1981. On Basin Hypsometry and the Morphodynamic Response of Coastal Inlet Systems. *Marine Geology*, v.40, pp 27-48.
- BRUUN, P., 1968. *Tidal Inlets and Littoral Drift*. University Book Company, Oslo, Norway.
- CHEN, C.L., 1994. Closure of "Momentum and energy coefficients based on power-law velocity profile": *Journal of Hydraulic Engineering*, American Society of Civil Engineers, v. 120, no. 5, p. 669.
- CLEARY, W. J. 1996. Inlet induced shoreline changes: Cape Lookout-Cape Fear, In Cleary (ed), *Environmental Coastal Geology: Cape Lookout to Cape Fear, NC*, Carolina Geological Society, p. 49-58.
- CLEARY, W.J., 2001. Inlet-Related Shoreline Changes: Rich Inlet, North Carolina, Final Report, *Figure Eight Beach Homeowners Association*, Wilmington, NC, 35 p. and appendices.
- CLEARY, W.J. and HOSIER, P.E., 1979. Coastal Geomorphology Washover History and Inlet Zonation: Cape Lookout, North Carolina to Bird Island, North Carolina. In Leatherman, S.D., *Barrier Islands: From the Gulf of St. Lawrence to the Gulf of Mexico*, p. 237-262.

- CLEARY, W.J. and HOSIER, P.E., 1993. *Natural and anthropogenic inlet induced shoreline change in southeastern North Carolina*. Large Scale Coastal Behavior 1993, U.S. Dept. of Interior, USGS Open File Report 93-381, p. 37-40.
- CLEARY, W.J. and MARDEN, T.P., 1999. *Shifting Shorelines: A Pictorial Atlas of North Carolina Inlets*, UNC SG-99-04, Raleigh, NC, 51 p.
- DILORENZO, J.L., 1988. The overtide and filtering response of small inlet/bay systems. In Aubrey, D.G., Weishar, L. *Hydrodynamics and sediment dynamics of tidal inlets: lecture notes on coastal and estuarine studies 29*. Springer Berlin Heidelberg New York, pp. 24-53.
- ESCOFFIER, F.F., 1940. The Stability of Tidal Inlets. *Shore and Beach*, V. 8 No. 4, p. 114-115.
- FITZGERALD, D.M., 1996. Geomorphic Variability and Morphologic and Sedimentologic Controls of Tidal Inlets, *Journal of Coastal Research, Special Issue*, No.23 p. 47 - 71.
- FITZGERALD, D.M. and NUMMEDAL, D., 1983. Response characteristics of an ebb dominated tidal inlet channel. *Journal of Sedimentary Petrology*, 53, pp. 833-845.
- FOLK, R.L. and WARD, W.C. 1957. Brazos River bar: a study in the significance of grain size parameters. *Journal of Sedimentary Petrology* 27, pp. 3-26.
- HAYES, M. O., 1980. General Morphology and Sediment Patterns in Tidal Inlets. *Sedimentary Geology*, 26, pp.139-156.
- HAYES, M.O., 1994. The Georgia Bight barrier system: In Davis (ed), *Geology of Holocene Barrier Islands Systems*, Springer Verlag, Chapter 7, p. 233-305.
- JACKSON, C.W. and CLEARY, W.J., 2003. Oceanfront changes associated with channel repositioning in a stable inlet system: Rich Inlet, NC, USA, *Proceedings of Coastal Sediments '03*, American Society of Civil Engineers, New York, NY.
- JACKSON, C.W., 2003. Personal Communication. University of North Carolina at Wilmington, Center for Marine Science. Wilmington, NC.
- JARRETT, J.T., 1976. *Tidal Prism-Inlet Area Relationships, Report 3*. USACE General Investigations of Tidal Inlets.

- JARRETT, J.T. 1977. Sediment Budget Analysis, Wrightsville Beach to Kure Beach, NC, *Proceedings of Coastal Sediments '77*, American Society of Civil Engineers, New York, NY, pp. 986-1005.
- JOHNSEN, C.D., CLEARY, W.J., FREEMAN, W.C., and SAULT, M., 1999. Inlet Induced Shoreline Changes on the High Energy Flank of the Cape Fear Foreland, NC. *Coastal Sediments 99* ASCE, New York, NY, pp. 1402-1418.
- KEULEGAN, G.H., 1951. Tidal Flow in Entrances, Water Level Fluctuations of Basins in Communication with Seas, *Report No. 1146*, National Bureau of Standards.
- LANGFELDER, L.J., FRENCH, T., MCDONALD, R., and LEDBETTER, R., 1974. A Historical Review of Some of North Carolina's Coastal Inlets. Center for Marine and Coastal Studies, NCSU, Raleigh, NC. *Report No. 74-1*, 43 p.
- LINCOLN, J.M. and FITZGERALD, D.M., 1988. Tidal Distortions and Flood Dominance at Five Small Tidal Inlets in Southern Maine. *Marine Geology*, v. 82, pp. 133-148.
- MARINO, J.N. and MEHTA, A.J., 1987. Inlet Ebb Shoals Related to Coastal Parameters. *Proceedings Coastal Sediments '87*, ASCE, 1608-1623.
- MANNING, R., 1891. *On the Flow of Water in Open Channels and Pipes*. Transactions of the Institution of Civil Engineers of Ireland.
- MCNINCH, J.E., 2003. *Letter Report: Mean Current Flow Across the Mouth of the Cape Fear River Tidal Inlet and the New Channel Region, 2002*.
- MCNINCH, J.E., 2003. *Letter Report: Mean Current Flow Across Oregon Inlet, North Carolina, 2003*.
- MILITELLO, A., and KRAUS, N. C., 2001. Shinnecock Inlet, New York, Site Investigation, Report 4, Evaluation of Flood and Ebb Shoal Sediment Source Alternatives for the West of Shinnecock Interim Project, New York. Coastal Inlets Research Program, *Technical Report ERDC-CHL-TR-98-32*. U. S. Army Engineer Research and Development Center, Vicksburg, Mississippi.
- MOTA OLIVEIRA, I.B., 1970. Natural Flushing Ability of Tidal Inlets. *Proceedings of Conference of Coastal Engineering, 12th*. American Society of Civil Engineers, pp. 1827-1845.

- NAYAK, I.V., 1971. *Tidal Prism – Area Relationship in a Model Inlet*. Technical Report HEL 24-1, Hydraulic Engineering Laboratory, University of California at Berkeley, Berkeley, CA.
- NUMMEDAL, D.N., OERTEL, G.F., HUBBARD, D.K., and HINE, A.C., 1977. Tidal Inlet Variability - Cape Hatteras to Canaveral, *Proceedings of Coastal Sediments, '77*, American Society of Civil Engineers, Charleston, SC., p. 543-562.
- O'BRIEN, M.P., 1969. Equilibrium Flow Areas of Inlets on Sandy Coasts. *Journal of the Waterways and Harbor Division*, ASCE, v. 95 (WW1), p. 43-52.
- PULAWSKA, A., 1999. WinRiver software. RD Instruments. rdinstruments.com.
- SEABERGH, W.C., 2003. Engineering Analysis at Tidal Inlets. *4th Annual Tech –Transfer Workshop, Session H-2*.
- US Army Corps of Engineers, 1982. *Feasibility Report and Environmental Assessment of Shore and Hurricane Wave Protection, Wrightsville Beach, North Carolina*, Wilmington District Office, Wilmington, NC.
- U.S. Army Corps of Engineers, 1999. *Manteo (Shallowbag) Bay, North Carolina, General Design Memorandum and Environmental Impact Statement, Supplement No. 2*, Wilmington District Office, Wilmington, NC.
- U.S. Army Corps of Engineers, 2003. *Database of Federal Inlets and Entrances*. Coastal Inlet Research Program, <http://cirp.wes.army.mil/cirp/cirp.html>.
- VALLIANOS, L., 1975. A Recent History of Masonboro Inlet, North Carolina. Cronin, L.E., ed., *Estuarine Research*, Volume II Geology and Engineering, NY Academic Press, p. 151-166.
- VAN DE KREEKE, J., 1967. Water Level Fluctuations and Flow in Tidal Inlets, *Journal of the Waterways and Harbor Division*, ASCE, V. 93 (WW4), p.97-106.
- WALTON, T.L. and ADAMS, W.D., 1976. Capacity of Inlet Outer Bars to Store Sand. *Ch. 12, Proceedings, 15th International Conference on Coastal Engineering*, ASCE, p. 1919-1937.
- WATERWAY SURVEYS AND ENGINEERING (WSE), Ltd., 2001. Rudee Inlet Management Study. Virginia Beach, Virginia.
- WELSH, J., 2003. Personal Communication. University of North Carolina at Wilmington, Center for Marine Science. Wilmington, North Carolina.

ZARILLO, G. A. and MILITELLO, A., 1999. Ponce de Leon Inlet, Florida, Site Investigation. Report 2: Inlet Hydrodynamics: Monitoring and Interpretation of Physical Processes. *Technical Report CHL-99-1*. U. S. Army Engineer Waterways Experiment Station, Vicksburg, Mississippi.